Contact Tube Temperature during GMAW

Understanding what increases its temperature can help lengthen a contact tube's operational life

BY G. ADAM, T. A. SIEWERT, T. P. QUINN, AND D. P. VIGLIOTTI

In gas metal arc welding (GMAW), a spool continuously feeds an electrode through a contact tube that positions and transfers current to the electrode. The contact tube is usually made of a copper alloy because the material has good thermal and electrical conductivity. Contact tube failure results when the tube hole grows to where the tube can no longer accurately direct the electrode, when the tube provides intermittent or no current to the electrode, or when the tube-electrode interface causes electrode velocity to fluctuate or stop. The first two failure modes occur when sliding contact causes wear and the hole in the contact tube increases in size. The third failure mode occurs when debris builds up on the tube's interior until mechanical interference between the electrode and tube hinders the electrode feed and causes the arc to become unstable. In all cases, stick-slip mechanisms can cause variations in an electrode's feed speed, making the arc unstable (Refs. 1, 2).

As wear enlarges the hole in the tube, the electrode can suddenly shift contact points, causing intermittent contact, at the least, or arcing inside the tube, at the worst. Arcing could weld the electrode to the tube, causing the electrode to stop and the arc length to increase until the contact tube melts. If debris or dirt accumulates in the contact tube, wire-feed speed (WFS) can fluctuate, resulting in arc instability. Spatter accumulated on the contact tube face that narrows or closes the hole for the electrode is another common cause of failure.

Each mechanism that causes contact-tube failure worsens as temperature rises. Wear also increases with higher temperatures (Refs. 3, 4). The object of this article is to understand the important heating and cooling mechanisms of the contact tube.

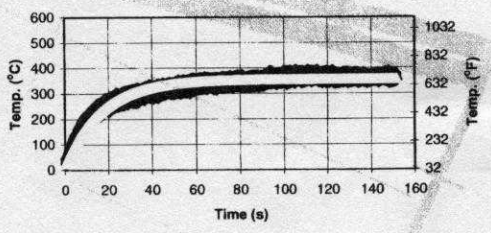

Fig. 1 — A typical heating curve for a contact tube during a weld.

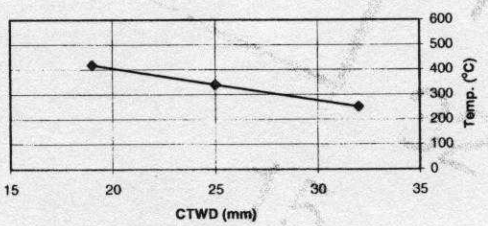

Fig. 2 — Average (over all voltages and electrode feed speeds) equilibrium contact tube temperature vs. CTWD.

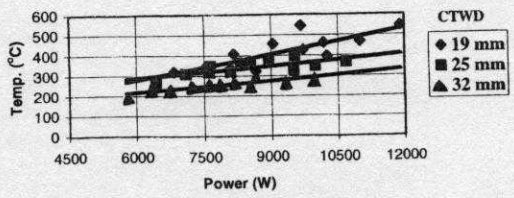

Fig. 3 — Equilibrium temperature vs. power for various CTWD values.

G. ADAM, T. A. SIEWERT, T. P. QUINN, and D. P. VIGLIOTTI are with NIST, Boulder, Colo.

Table 1 — Approximate Heat Transferred to and from the Contact Tube at Equilibrium

Mechanism	Assumptions	Heat Transfer
Resistive heating from voltage drop at interface between electrode and contact tube	Half of the heat generated goes into the contact tube. I = 200 to 450 A, voltage drop at interface is 0.5 V	50 to 110 W
Ohmic heating from the current as it passes the length of the contact tube	Pure copper contact tube at 669 K I = 365 A	6 W
Radiative heating on the face of the contact tube	The contact tube is a gray-body emitter/absorber at 667 K. The arc is a black-body emitter at 13,437 K (Ref. 6). The arc is modeled as a disk 32 to 19 mm away from the contact tube with a diameter of 9 mm (Ref. 6).	21 to 68 W
Convective cooling of the contact tube as the argon flows along its length	Constant heat flux from the contact tube, which is at a uniform temperature of 667 K. The argon enters at a temperature of 294 K and has a Prandtl Number of 0.7 and a thermal conductivity of 0.018 W/(m K) (Ref. 7). The thermal properties for the argon are taken at the average temperature. No heat transfer to the gas cup.	–6 W
Conduction of heat along the contact tube into the rest of the gun.	The contact tube transfers heat to the gun body, which is maintained at 290 K. The tip of the contact tube is at 460–670 K.	–65 to –130 W

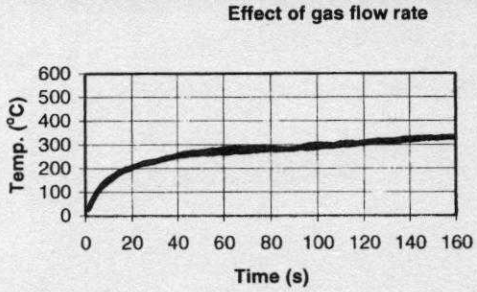

Fig. 4 — Effect of gas flow rate on the contact tube's heating curve.

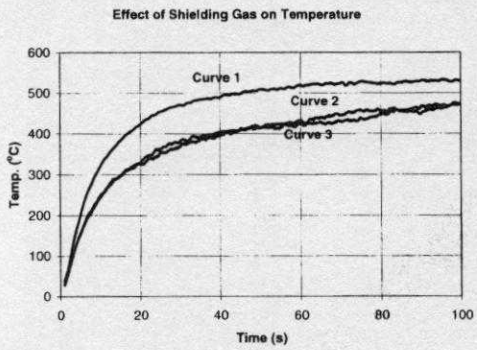

Fig. 5 — Effect of shielding gas composition on the contact tube's heating curve. The welding parameters for each curve are detailed in Table 3.

Heat Flux

Heat input to the tube comes primarily from the following sources:

◆ Radiation from the arc and weld pool. As long as the arc is stable, this source is approximately constant in time and depends primarily on contact-tube-to-work distance (CTWD) and secondarily on arc length. There is also a small amount of radiation from the weld pool.

◆ Resistive heating at the interface as current is transferred between the contact tube and welding electrode.

◆ A small amount of ohmic heating due to current flowing through the contact tube (Refs. 4, 5).

◆ A negligible amount of heat conducts upward through the welding electrode from the weld.

The following processes cool the contact tube during welding:

◆ Conduction of heat to the upper parts of the gun.

◆ Convection via the shielding gas.

◆ Radiative losses, which are important only for very high contact tube temperatures.

Table 1 shows estimates for these heat sources and the assumptions used to develop them. The estimates were based on a 30-mm-long contact tube with a 6-mm O.D. and 1.6-mm I.D. The gas cup had a 15-mm I.D.

Estimates were developed for thermal equilibrium (after the temperature had stabilized) and balanced to within 10% of the experimental values. The radiation model considered the arc as a planar disk of constant temperature. The disk temperature was calculated as the average temperature over the volume of a 350-A arc (Ref. 8). Radiative transfer was considered only on the contact tube's face. The convection heat transfer model was for a not yet fully developed flow along a cylinder, either thermally or hydrodynamically. Changing conditions such as current, voltage, or CTWD changed the magnitude of these values, but estimates illustrated the relative effects of the various terms. The conductive terms were nearly linear with temperature and could be scaled to estimate the relative thermal flows for other conditions.

These estimates predicted that resistive heating and radiation dominated the other heating sources and balanced with cooling by conduction. The specific welding parameters used determined the ratio between resistive and radiation.

Experiments

For the experiment, a commercial air-cooled gun, inverter power source, and matching electrode feeder were used to make

Table 3 — Effect of Shielding Gas on the Contact Tube Temperature

Curve	Shielding Gas	Voltage, V	WFS, mm/s	Current, A	Power, kW
1	Ar-5%CO_2	29	140	410	12
2	CO_2	27	140	415	11
3	Ar-5%CO_2	26	130	430	11

bead-on-plate welds on 10-mm-thick x 50-mm-wide plates. The power source had pulsing capabilities, but the constant current mode was used to eliminate the complexities of pulse parameters. Older GMAW power sources typically have constant-voltage characteristics, and so offer a different response.

The contact tube had a mass of 9.5 grams and a heat capacity of 2.4 J/K, which meant a net heat input of about 100 W would produce an initial heating rate of 40°/s.

The electrode was AWS type E70S-3 and the shielding gas was an argon-5% CO_2 mixture, flowing at a rate of 18 L/min (40 ft³/h). One weld was made using 100% CO_2 to estimate the shielding gas effect. The air-cooled welding gun was rated at 400 A for CO_2 shielding gas and derated by the manufacturer to a 60% duty cycle for argon-based mixtures. The gun was fixed perpendicular to the plate, which was moved underneath at a constant speed of 7.75 mm/s (0.3 in./s). This speed, except for one test to examine speed effect, was maintained during all experiments. All weld runs lasted about 150 s, a time sufficient to reach thermal stability in the contact tube. Welding current and voltage were measured with a pair of isolated transducers to an absolute accuracy of 1 and 0.5%, respectively, and recorded on a personal computer. Contact tube temperature was measured with a K-type thermocouple inserted into a small hole at the side of the tube. The thermocouple's output, also recorded on the computer, was fed to a cold-junction-compensated linear amplifier that gave an analog output of 1.6 mV/°C. Sampling rate was 100 Hz.

To learn more about the contribution of radiation to contact tube heating, a number of welds were made with a ceramic radiation shield introduced between the contact tube and the workpiece. In this setup, a square of machinable ceramic (40 x 40 x 5 mm) was placed just below the contact tube. The welding electrode was fed through the ceramic square via a small hole drilled in its center. Three layers of ceramic cloth were placed between the ceramic radiation shield and the contact tube to eliminate any conduction between the two. In this setup, shielding gas was delivered to the weld area by an external tube. To demonstrate shielding can be achieved with more realistic welding conditions, some welds were made with a gas cup and ceramic shield. This shield was narrow enough to shield the contact tube from direct radiation while allowing gas flow to the weld area.

The experimental design was a full factorial matrix. Three CTWDs were used: 19, 25, and 32 mm (0.75, 1, and 1.25 in.). Shorter CTWDs were not investigated because room was needed for the ceramic radiation shield. Four wire-feed speeds were used: 110, 120, 130, and 140 mm/s (260, 285, 305, and 330 in./min). The voltages at the power supply were 27, 30, and 33 V, which corresponded to arc lengths of about 2, 4, and 6 mm, respectively. Some parameter combinations were well outside those normally used in welding, but the aim of this work was to analyze contact tube temperature over the widest possible range. This required a complete experimental matrix. To check the influence of the gas flow rate on contact tube temperature, two additional welds were made with gas flow rates of 14 and 23.6 L/min (30 and 50 ft³/h). To check the influence of welding travel speed on contact tube temperature, one weld was made at a speed of 15.5 mm/s (0.6 in./s).

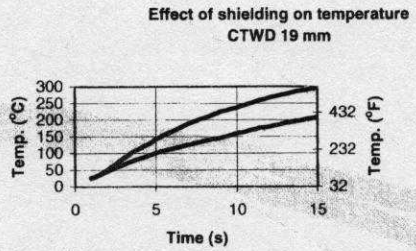

Fig. 6 — Effect of shielding on the contact tube's heating curve for CTWD of 19 mm. The top curve is unshielded and the lower curve is shielded.

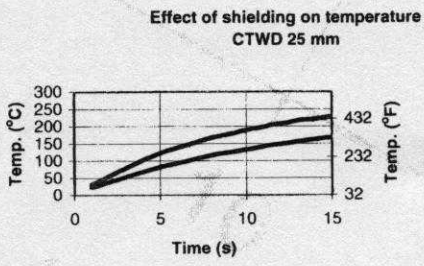

Fig. 7 — Effect of shielding on the contact tube's heating curve for CTWD of 25 mm. The top curve is unshielded and the lower curve is shielded.

Heating Model

A simple model was developed to simulate the contact tube's temperature rise with time. It was assumed the contact tube heats from a constant heat input (initially producing linear heating), and cools at a rate proportional to its temperature. The differential equation that describes such behavior is

$$dT/dt = k - \alpha T \quad (1)$$

where T is the temperature (°C), t the time (s), and k and α are constants.

Solving Equation 1 gives:

$$T(t) = k/\alpha + (T(0) - k/\alpha)e^{-\alpha} \quad (2)$$

According to this model, k/α is the temperature of the contact tube at very long times. For this work, T(t=0) was set at 24°C, the ambient temperature in the lab. To let the gun return to room temperature, a wait of 2.5 h minimum was held between welds. The constants k and α were varied to minimize the sum of the squares (R^2) of the difference between the measurements and the calculated curve. The R^2 of the fit was typically 0.94.

Table 2 — The Parameters and Results for All Welds

CTWD (mm)	Arc Length (mm)	Voltage Setting (V)	W. Speed (mm/s)	Average Voltage (V)	Average Current (A)	Final Temp (°C)	Heating Rate (°C/s)
19	2	27	110	20	350	319	17
19	2	27	120	22	340	340	20
19	2	27	130	24	331	336	20
19	2	27	140	27	323	322	22
19	4	30	110	21	391	408	24
19	4	30	120	24	381	455	32
19	4	30	130	26	372	427	22
19	4	30	140	28	365	396	25
19	6	33	110	22	436	544	36
19	6	33	120	24	429	461	29
19	6	33	130	26	419	466	28
19	6	33	140	29	410	544	40
25	2	27	110	18	356	265	15
25	2	27	120	21	346	309	19
25	2	27	130	22	339	316	20
25	2	27	140	24	332	318	21
25	4	30	110	19	398	347	20
25	4	30	120	21	390	364	22
25	4	30	130	23	382	372	24
25	4	30	140	25	375	398	25
25	6	33	110	19	446	355	16
25	6	33	120	22	436	323	22
25	6	33	130	23	431	349	20
25	6	33	140	25	423	367	24
32	2	27	110	16	365	195	7
32	2	27	120	18	358	236	12
32	2	27	130	20	348	256	14
32	2	27	140	21	347	239	14
32	4	30	110	16	409	225	11
32	4	30	120	18	402	245	12
32	4	30	130	21	394	269	14
32	4	30	140	22	388	293	16
32	6	33	110	17	454	244	12
32	6	33	120	19	447	251	15
32	6	33	130	21	439	273	13
32	6	33	140	23	433	289	16

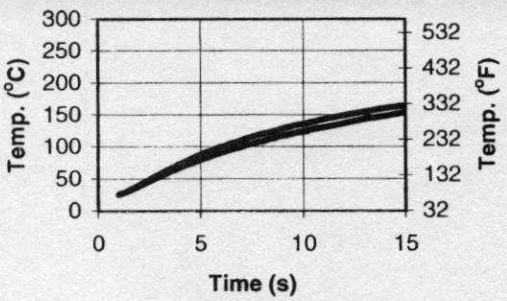

Fig. 8 — Effect of shielding on the contact tube's heating curve for CTWD of 32 mm. The top curve is unshielded and the lower curve is shielded.

Results and Discussion

Figure 1 shows temperature measurements for the contact tube during a weld. These 15,000 measurements (100 Hz for 150 s) show a band of data with a standard deviation about 14°C wide. Since the contact tube's mass was sufficient to damp small thermal fluctuations, the band's width was mainly due to electrical noise. The noise could not be filtered from the millivolt-scale thermocouple signal. Still, the temperature trend was quite clear. The band was wide enough to hide the model's prediction on this figure, which fits nicely down the center. Table 2 lists the main parameters and results for the welds that were performed. For the entire matrix, final temperatures ranged from 200 to 550°C (390 to 1000°F), and the temperature reached about 90% of the final value within 50 s. Initial heating rates (measured over the first 5 s) ranged from 6.6 to 40°C/s. At the high end of the final temperature range, the gas cup and contact tube were discolored. As expected, low temperatures and heating rates were obtained while welding with combinations of low WFS, low voltage (short arc length), and high CTWD, whereas high temperatures and heating rates were obtained for combinations of high voltage setting, high WFS, and low CTWD. For α, an average value of 0.059 s^{-1} was found with a standard deviation of 0.012 s^{-1}. Since changes in α were not correlated to changes in any weld parameters, α was fixed at 0.059 s^{-1}, and the model was fit to the data by varying just the final temperatures. The average effects of CTWD are presented in Fig. 2. As these effects are in descending order, they suggest radiation was a major heat source, especially at low CTWD values. This confirmed the heat transfer model data in Table 1. Figure 2 shows a reduction in radiation of 62% (68% increase in CTWD) reduces the equilibrium temperature by 40%.

Figure 3 shows the calculated final temperature as a function of average power (calculated from the measured current and voltage) and CTWD. This expressed heat input as power. As expected, lowering CTWD increased the temperature of the contact tube for a given input power.

Figure 4 shows the heating curves from two welds made with the same welding parameters but with two different gas flow rate values. One flow rate was 25% below that used for most of the test matrix, the other was 25% above. Even though flow rate was changed by 50%, the heating curves were almost identical and

reached the same final temperatures. This result was as predicted by the heat-transfer model, which indicated heat carried away by the gas was less than 10% of the total. Even a 50% change in gas flow rate had only a small effect on the heating curve.

Heating curves for two welds made with the same welding parameters but with different travel speeds (7.75 and 15.5 mm/s) were practically the same. This was explained by the fact the principal effect of the welding speed was on the size of the weld pool: the higher the travel speed, the smaller the weld pool. The weld pool contributes to heating of the contact tube mainly by radiation. It is further away from the tube than the arc. Since its temperature is only about 13% of that of the arc, the contribution of this heating is small. At these long CTWDs, changes in the size of the pool had minimal effect on the tube's heating curve.

Figure 5 demonstrates how selection of the shielding gas can affect heating of the contact tube. Curve 1 shows the temperature with Ar-5%CO_2, while curve 2 shows the temperature with CO_2 only, produced with the same welding parameters. The differences between these two welds demonstrate that switching to CO_2 resulted in lower contact tube temperature, while depositing the same amount of metal in the weld (same wire-feed speed of 140 mm/s). All weld parameter data for these welds are shown in Table 3. Changes between curve 1 and curve 2 can be explained by shielding gas effects on voltage and current (and total weld power). The model supports this result by indicating reductions in both resistive and arc-radiation contributions to contact tube heating, although the radiation effect appears to dominate here. No attempts were made to quantify the effects of the higher particulate level in the CO_2 arc or the change in the arc spectrum.

Curve 3 shows the temperature when wire-feed speed for the Ar-5% CO_2 weld was decreased until the arc power was the same as for the weld with CO_2 (curve 2). Here, the temperatures of the contact tubes with the two shielding gases followed nearly identical patterns. Thus, the lower tube temperature for the weld with CO_2 at the same power source settings seems most related to the reduction in arc power. Since the current increased while the voltage decreased, the relative changes in the contributions from resistive heating and arc radiation seem to offset each other. Good arc length measurements for the shielding gas tests could not be obtained, so no comparisons were made between these changes and the heat estimates. In general, using CO_2 as a shielding gas enables one to deposit more metal into the weld for a given temperature rise in the tube.

A solid ceramic radiation shield and a few layers of ceramic cloth placed between the arc and contact tube effectively eliminated radiative heating, separating this effect from other heat sources. Note the ceramic became red hot even during these short tests and often cracked during cooling. This further supports the intensity of the radiation from the arc. Figures 6–8 show the heating curves (with and without the heat shield in place) for CTWD values of 19, 25, and 32 mm, respectively. The contribution of radiation from the arc was very pronounced at a CTWD of 19 mm and much smaller at 32 mm. The significant drop in the relative contribution of radiation with distance for the examples in Figs. 6–8 confirms the trends shown in Fig. 2 for the averages of the entire test matrix. Figure 6 shows a 33% reduction in equilibrium temperature when the radiation contribution was eliminated by the ceramic shield. This was close to the 40% reduction in equilibrium temperatures found for the test matrix averaged in Fig. 2. The exact ratios of the contributions of radiation and resistive heating obviously depend on the welding conditions; however, these tests show these contributions can be similar in magnitude.

To fit the ceramic shield and cloth against the contact tube for the tests in Fig. 6–8, the gas cup had to be removed. This meant the shielding gas had to be fed from the side, an arrangement that was convenient for the tests but could be criticized as not accurately simulating actual situations. To come closer to standard practice, another weld was tried with the gas cup in place and a smaller (about 25 x 25 mm) ceramic shield just below it. This smaller shield had a series of holes for the usual axial flow of shielding gas, but the holes also allowed a small amount of radiation to reach the contact tube. This compromise in design meant the tube was expected to heat a little faster than it would with the higher-quality radiation shielding used for Figs. 6–8. After a few seconds, the narrow shield started to melt. This was not surprising because it was mounted on the bottom of the gas cap, much nearer to the arc. As the shield melted, radiation from the arc was able to reach the contact tube, so the heating curve slowly approached the unshielded curve. This experiment demonstrated that radiative shielding can be achieved under normal welding conditions, but it is difficult to develop a shield that can withstand the intense heat of the arc.

Summary

The contact tube in an air-cooled GMAW gun often reaches a temperature of 300°C (570°F) or higher for typical welding conditions, nearly halfway to the melting temperatures of many common copper alloys. The contact tube reaches about 90% of its equilibrium temperature in about 50 s. This means higher power inputs can be tolerated for short welds (10–20 s) because the contact tube never reaches the equilibrium temperature. Figure 2 confirmed equilibrium temperature goes down with increasing CTWD, but up with WFS and welding voltage. Over the measured range, WFS has the least influence on final temperature. This means that, without overheating of the contact tube, the power input to the weld can be increased by increasing the voltage and the WFS, provided the CTWD is also increased. This is also demonstrated in Fig. 3, which shows how to move along a constant temperature (horizontal) line by increasing power and CTWD at the same time.

Radiation from the arc and resistive heating from the electrode-contact tube interface are two major sources of contact-tube heating. Shielding the contact tube from arc radiation can reduce its temperature significantly, especially at low CTWD values, and lengthen its operational lifetime. Conduction of heat into the gun body through the contact tube mount is the most important means of cooling the contact tube. Cooling from shielding gas flowing around the contact tube provides only about 10% of the conductive cooling effect.◆

References

1. Quinn, T. P., Madigan, R. B., Mornis, M. A., and Siewert, T. A. 1995. Contact tube wear detection in gas metal arc welding. *Welding Journal* 74(4): 115-s to 121-s.

2. Quinn, T. P., Madigan, R. B., and Siewert, T. A. 1994. An electrode extension model for gas metal arc welding. *Welding Journal* 73(10): 241-s to 248-s.

3. Rabinowicz, E. 1982. The temperature rise at sliding electrical contacts. *Wear* 78: 29–37.

4. Villafuerte, J. 1999. Understanding contact tip longevity for gas metal arc welding. *Welding Journal* 78(12): 29–35.

5. Yamada, T,. and Tanaka, O. 1987. Fluctuation of the wire feed rate in gas metal arc welding. *Welding Journal* 66(9): 35–42.

6) Sparrow, E. M., and Cess, R. D. 1978. *Radiation Heat Transfer.* Washington: Hemisphere Publishing Corp., p. 340.

7) Kays, W. M., and Perkins, H. C. 1985. *Handbook of Heat Transfer Fundamentals*, eds. W. M. Rohsenow, J. P. Hartnett, and E. N. Ganic. New York, N.Y.: McGraw Hill, pp. 7-47 to 7-88.

8) Jonsson, P .G., Szekely, J., Madigan, R. B., and Quinn, T. P. 1995. Power characteristics in GMAW: Experimental and numerical investigation. *Welding Journal* 74(3): 93-s to 101-s.

9. *Welding Handbook*, Vol. 2 (Welding Processes), 8th ed. 1991. Miami, Fla.: American Welding Society, p. 14.